

SPICE Model of Mutlu-Kumru Memristor Model and Its Usage for Analysis, Modeling, And Simulation of a Memristor-Based Sawtooth Signal Generator

Ertuğrul KARAKULAK^{1*}, Reşat MUTLU²

¹ Electronics Department, Vocational School of Technical Sciences, Tekirdağ Namık Kemal University, Tekirdağ, Türkiye

² Electrical and Electronics Engineering Department, Çorlu Engineering Faculty, Tekirdağ Namık Kemal University, Çorlu, Tekirdağ, Türkiye

Cite this article as: Karakulak, E., Mutlu R. (2024). Spice Model of Mutlu-Kumru Memristor Model and Its Usage for Analysis, Modeling, And Simulation of a Memristor-Based Sawtooth Signal Generator, *Trakya University Journal of Engineering Sciences*. 25(2), 91-100.

Highlights

- SPICE Model of the Mutlu-Kumru Memristor Model
- Sawtooth Signal Generator Simulation with the Mutlu-Kumru Model
- Sawtooth Signal Generator Analysis with the Mutlu-Kumru Model

Article Info	Abstract
Article History: Received: September 16, 2024 Accepted: December 23, 2024	Memristor has turned into a popular nonlinear circuit element following the discovery of a thin-film system that mimics the behavior of a memristor. Some memristor research has concentrated on developing new memristor models. Some memristor models have window functions. In the literature, there are a lot of different window functions proposed for modeling them. Recently, it has been shown that some memristive models cannot do a complete resistive switching in a finite time and a window function with a finite resistive switching time has been suggested to model a memristor. In this paper, its Spice model has been given. The model is modified using a different shaping factor for each polarity. Its Spice model is made in the LTspice program. As an example, the model is used to simulate a memristor-based sawtooth generator in this study. Its simulation results are also presented to verify the circuit's operation as a sawtooth signal generator.
Keywords: Memristor; Memristor Model; Sawtooth Signal Generator; Window Function.	

Mutlu-Kumru Memristör Modelinin SPICE Modeli ve Testeredişi Sinyal Jeneratörü İçin Analizi, Modellenmesi ve Simülasyonu

Makale Bilgileri	Öz
Makale Tarihiçesi: Geliş: 16 Eylül 2024 Kabul: 23 Aralık 2024	Memristor, memristörün davranışını taklit eden ince film sisteminin bulunmasından sonra popüler bir doğrusal olmayan devre elemanına dönüşmüştür. Memristör araştırmalarından bir kısmı yeni memristör modellerinin geliştirilmesi üzerinde yoğunlaşmıştır. Bazı memristör modelleri pencere fonksiyonlarına sahiptir. Literatürde memristörlerin modellenmesi için önerilen birçok farklı pencere fonksiyonu bulunmaktadır. Son zamanlarda, bazı hafızalı modellerinin sonlu bir zamanda tam bir rezistif anahtarlama yapamadığı gösterilmiş ve bir memristörü modellemek için sonlu rezistif anahtarlama zamanlı bir pencere fonksiyonu önerilmiştir. Bu yazıda bu modelin Spice modeli verilmiştir. Model, her polarite için farklı bir şekillendirme katsayısı kullanılarak değiştirilebilmektedir. Spice modeli LTspice programında yapılmıştır. Bu çalışmada örnek olarak, bu model memristör-tabanlı bir testere dişi jeneratörünü simüle etmek için kullanılmıştır. Simülasyon sonuçları devrenin testere dişi jeneratörü olarak çalıştığını doğrulamak için verilmiştir.
Anahtar Kelimeler: Memristör; Memristör Modeli; Testere Dişi Sinyal Üretici; Pencere Fonksiyonu.	

1. Introduction

The claim for the memristor's existence was made in 1971 (L. O. Chua, 1971). In 1976, memristive systems and their properties have been described (L. O. Chua & Kang, 1976). In 2008, a thin-film memristive system that behaves as a memristor has been discovered (Strukov et al., 2008). In the last decade, memristor and memristive systems have become hot research areas (Pershin et al., 2011; Prodromakis & Toumazou, 2010). New materials in nano dimensions showing memristive properties are under research (Pershin & Di Ventra, 2011). Memristor is expected to be used in analog and digital circuit applications (L. Chua, 2011; Prodromakis & Toumazou, 2010). That's why it is important to develop memristor models (Khalid, 2019). Because of their non-linear nature, it is hard to model the electrical characteristics of the memristors. Memristor models that have window functions are commonly used to model memristors and there are various window functions in the literature (D. Biolek & Biolková, 2009; Eroğlu, 2017; Joglekar & Wolf, 2009; Khalid, 2019; Prodromakis et al., 2011; Strukov et al., 2008; Zha et al., 2016). The first window function is presented by Strukov et al (Strukov et al., 2008). Joglekar has also provided a shapeable nonlinear dopant drift memristor model but it has a boundary-tackling issue (Joglekar & Wolf, 2009). Biolek et al have given a current direction-dependent window function without any boundary-tackling issues (D. Biolek & Biolková, 2009). Prodromakis et al have given a scalable and shapeable window function but with a boundary-tackling issue (Prodromakis et al., 2011). The model has been modified to get rid of the boundary-tackling issue and to have scalability (Zha et al., 2016). Some of the models are phenomenological approaches (Eroğlu, 2017; Khalid, 2019). In (Mutlu & Kumru, 2023), a boundary unreachability issue has been shown to exist for some memristor models, i.e., they do not switch in a finite time.

TEAM memristor model, which is a general model, simplifies the Simmons Tunnel Barrier Model and the derivative of its state space function is given as a piecewise function (Kvatinsky, S., et al., 2012). It makes use of thresholds in the model. An exponential function-based window function, which still suffers from boundary-tackling issues, has been suggested (Oğuz, Y., et al., 2017). Some memristor models have piecewise linear window functions (Hernández et al, 2019; Karakulak et al., 2020). A new window function, which provides finite resistive switching times has been reported in (Mutlu & Kumru, 2023). The model is also simple enough to provide some analytical solutions for resistive switching times.

Memristors may allow programmable electronic circuits made (Shin et al., 2009, 2011). Electronically programmable amplifiers can be made with memristors (Berdan, R.; Prodromakis, T.; Toumazou, 2012; Pershin & Di Ventra, 2010; T. a. Wey & Jemison, 2011). Memristor-based filters have been examined in the literature (Ascoli et al., 2013; S. C. Yener et al., 2018; Ş. Ç. Yener et al., 2014). It is possible to make memristor-based phase shifters or modulator circuits (Mutlu, R., Karakulak, 2018; T. A. Wey & Benderli, 2009). In (Itoh & Chua, 2008; Muthuswamy, 2010), memristor-based chaotic oscillators are examined. In (Mosad et al., 2013; Mutlu, 2015; Talukdar et al., 2011; S. Ç. Yener et al., 2014), different types of memristor-based relaxation oscillators are presented.

A memristor-based sawtooth signal generator (MBSSG) is suggested and examined analytically and experimentally using an HP memristor emulator (Özgülvenç et al., 2016). Other memristor models with nonlinear drift speed are also used to simulate the MBSSG (Kurt Demir A.; Mutlu R., 2019). It is shown that the memristor models used in (Kurt Demir A.; Mutlu R., 2019) have either boundary tackling or boundary reachability issues except for the HP memristor model (Mutlu & Kumru, 2023). Although

the simulations of the MBBSG are made in (Kurt Demir A.; Mutlu R., 2019), the nonlinear dopant drift memristor models cannot complete the resistive switching analytically and therefore the simulations are wrong (Mutlu & Kumru, 2023). The model given by Kumru and Mutlu can be used to model the MBBSG since such a memristor model completes a resistive switching in both forward and reverse polarities as the model since it does not have any boundary tackling and unreachability issues. The study aims to analyze the MBSSG with the new model, give its LTspice of model (Mutlu & Kumru, 2023), and use it to simulate the MBSSG.

This paper is arranged in the following way. In the second section, the Mutlu-Kumru memristor model is briefly told. In the third section, its LTspice model is given. In the fourth section, the MBSSG is given and its LTspice simulations are given. The paper is finished with the conclusion section.

2. Mutlu-Kumru Memristor Model

Some thin films, that have frequency-dependent zero-crossing hysteresis loops, are memristive systems and are nowadays called memristors. Such a memristor model with nonlinear dopant drift is presented as

$$v(t) = R(x)i(t) \quad (1)$$

$$\frac{dx}{dt} = \mu_v \frac{R_{on}}{D^2} \cdot i(t)f(x, i) \quad (2)$$

where $R(x)$ represents the resistance of the memristor, $i(t)$ denotes its current, $v(t)$ indicates its voltage, w is the length of its oxidized region, μ_v is the dopant mobility, D is the total length of the TiO_2 region, $x=w/D$ is the normalized oxidized length, R_{on} is the minimum resistance, and $f(x, i)$ is the window function.

The resistance of the memristor is given as

$$R(x) = R_{off} - (R_{off} - R_{on})x \quad (3)$$

HP memristor does. Some LTspice models of memristors are available in the literature (D. Biolek & Biolková, 2009; Karakulak & Mutlu, 2020). A memristor-capacitor (M-C) parallel circuit is inspected with an LTspice model of the proposed memristor model, but the model was not presented in (Mutlu & Kumru, 2023). It is important to present its LTspice

Its resistance varies between its minimum value, R_{on} , and its maximum value, R_{off} .

A window function indicates how closely a memristive system approximates an ideal memristor (Z. Biolek et al., 2009). The resistance value or memristive state-variable changes only when the window function $f(x, i)$ is not equal to zero. In (Mutlu & Kumru, 2023), it is shown that some of the well-known models also have another problem named boundary reachability issue, i.e., their memristive switching time takes infinite time in both polarities and a new window function which also depends on device polarity is suggested:

$$f(x, i) = m_1 \sqrt[n]{1-x} \cdot stp(i) + m_2 \sqrt[n]{x} \cdot stp(-i). \quad (4)$$

where n is a positive number used to shape the window function, and, m_1 and m_2 are scaling parameters for the forward and reverse polarities respectively.

A memristor model with this window function switches in finite time when a DC voltage is applied (Mutlu & Kumru, 2023). Such a window function can be modified to have two shaping parameters, one for each direction:

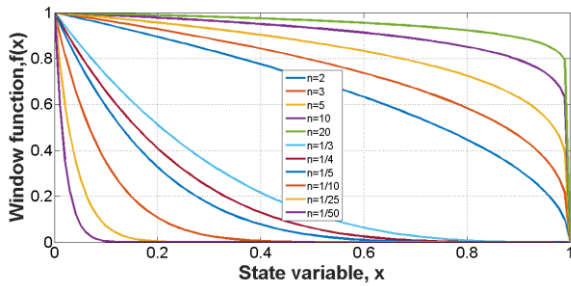
$$f(x, i) = m_1 \sqrt[n_1]{1-x} \cdot stp(i) + m_2 \sqrt[n_2]{x} \cdot stp(-i). \quad (5)$$

where n_1 and n_2 are the shaping parameters for the forward and reverse polarities respectively.

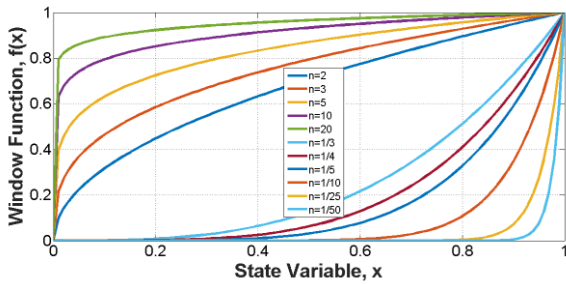
The new function can also be expressed as a piecewise function:

$$f(x, i) = \begin{cases} m_1 \sqrt[n_1]{1-x}, & i \geq 0 \\ m_2 \sqrt[n_2]{x}, & i < 0 \end{cases} \quad (6)$$

Combining Eq.s (1-5) makes the new memristor model. The plots of Mutlu-Kumru window functions for the forward and reverse polarities are given in Figure 1. The shaping parameters n_1 and n_2 defines the shape of the window functions. More information about the model can be found in (Mutlu & Kumru, 2023).



(a)



(b)

Figure 1. The Mutlu-Kumru window function for a) the forward biased memristor ($i(t) > 0$), various n_1 values, and $m_1=1$ and b) the reverse biased memristor ($i(t) < 0$), various n_2 values, and $m_2=1$.

3. Memristor Spice Model With The Mutlu-Kumru Model

The new memristor model is made in the LTspice simulator environment since it is a program that has also been often used to make lots of the memristor models given in the literature. The LTspice code of the new model is presented in Table 1. The block scheme of the memristor model is shown in Figure 2. The current source placed between the input nodes whose

current is equal to $i_{mem}(i(t))$ is used to represent the memristor and the other current source and a capacitor is utilized to calculate the state variable of the memristor ($x(t)$). This memristor model possesses three pins or nodes. The pin XSV lets the state variable of the memristor be plotted. The model is simulated with a sinusoidal voltage for three different frequencies. Its hysteresis curves are plotted together to illustrate that it possesses the three fingerprints of a memristor as seen in Figure 3. The Lissajous curves are not symmetric with respect to the origin due to their polarity dependence and differing scaling parameters. Memristor waveforms for 20 Hz are shown in Figure 4.

Table 1. Memristor Model Codes

```
* SPICE Model of Mutlu-Kumru Memristor
* TE: Top electrode
* BE: Bottom electrode
* XSV: External connection to plot state variable

.SUBCKT MEM_MK TE BE XSV
.param Ron=150 Roff=1000 x0=0.076 D=16N uv=40F
m1=2 m2=3 n1=2 n2=2
* The Current Polarity Dependent Window Function a
.func fa(V1)={m1*pow(V1,1/n1)}
* The Current Polarity Dependent Window Function b
.func fb(V1)={m2*pow((1-V1),1/n2)}
* Window Functions with respecting to current direction
.func f(V1,V2)={stp(V2)*fb(V1)+(1-stp(V2))*fa(V1)}
* Memristor I-V Relationship
.func IVRel(V1,V2) = V1/(Ron*V2 + Roff*(1-V2))
* Circuit to determine state variable
Gx 0 XSV
value={I(Gmem)*Ron*uv*f(V(XSV,0),I(Gmem))/pow(D,2)}
Cx XSV 0 {1}
.ic V(XSV) = x0
* Current source representing memristor
Gmem TE BE value={IVRel(V(TE,BE),V(XSV,0))}
.ENDS MEM_MK
```

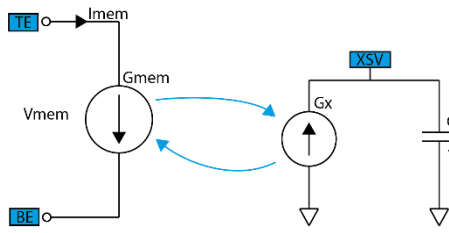


Figure 2. Block Scheme of Memristor Model

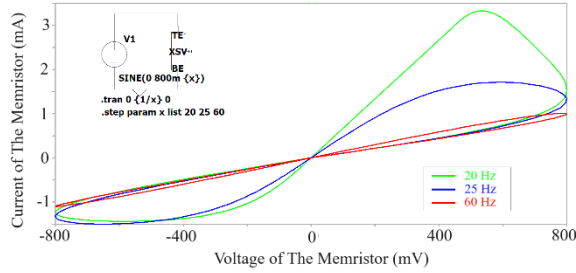


Figure 3. Hysteresis curves of the simulated memristor fed by a sinusoidal voltage of $V_s(t)=0,8\sin(2\pi ft)$ V for the frequencies of 20, 25, and 60 Hz.

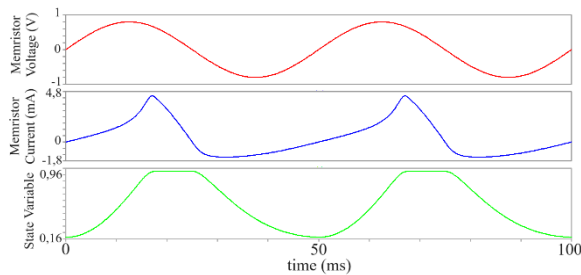


Figure 4. Voltage, Current, and State variable curves of the Mutlu-Kumru memristor model for 20 Hz.

4. Simulation Results

The memristor-based sawtooth signal generator (MBSSG) presented in (Özgüvenç et al., 2016) is shown in Figure 5. It comprises a relaxation oscillator and an inverting amplifier that has a memristor used as the feedback component. The purpose of the relaxation oscillator is to produce a square wave. In Figure 4, the memristor polarity is selected so that its memristance increases with a positive current. The input current of the R-M amplifier is also the memristor current. The square wave results in the opamp being fed by a square wave current. Memristor's memristance decreases in the positive alternance and increases in the negative

alternance if the memristor is not under saturation, i.e., its state variable is varying. In this case, the output of the MBSSG generator is negative memristor voltage. If the memristor is under saturation, i.e., its state variable is constant, the output of the MBSSG generator becomes constant, too. The output voltage of the relaxation generator can be assumed to be

$$V_{in} = \begin{cases} V_{sat}, & 0 < t < \frac{T}{2} \\ -V_{sat}, & \frac{T}{2} < t < T \end{cases} \quad (7)$$

Where V_{sat} is the saturation voltage of the opamp of the relaxation oscillator and T is the electrical period of the square wave and equal to $1/f$.

The frequency of the relaxation oscillator is given as

$$f = \frac{0.455}{R_f C} \quad (8)$$

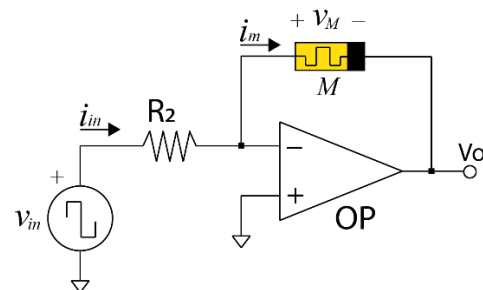
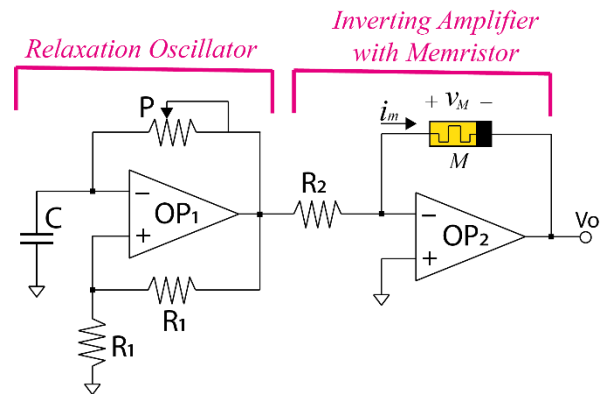


Figure 5. The sawtooth wave generator with a memristor (Özgüvenç et al., 2016).

LTspice circuit presentation of the MBSSG is given in Figure 6 and it is analyzed using the Mutlu-Kumru

memristor model made in the last section. The memristor parameters used in the simulations are given in Table 1. For various memristor parameters, the output voltage waveform is presented in Figures 7-10.

Table 2. Circuit element parameters used in simulations

The memristor minimum resistance	R_{on}	150 Ω
The memristor maximum resistance	R_{off}	1000 Ω
The dopant mobility	μ_v	40.10^{-15} $m^2/V.s$
The memristive element length	D	16 nm
Parameter m_1	m_1	2
Parameter m_2	m_2	3
Parameter n_1	n_1	2
Parameter n_2	n_2	2

The MBSSG generator circuit has been simulated for three different frequencies: 20, 50, and 250 Hz. The frequency dependence of the shape of the output voltage of the MBSSG generator in the steady-state can be seen in the simulation results given in Figures 7-9. 20 Hz operation frequency is low enough for the memristor to get into saturation since its voltage becomes constant in some intervals in each period. Due to the operation of the memristor in the saturation region, the output voltage is not a sawtooth waveform. When the frequency is increased to 50 Hz, the period is not long enough for memristor to get into saturation, the memristor output voltage resembles a sawtooth waveform more. At 250 kHz, the period is shorter and the memristor's memristance only varies just a little bit and almost stays constant, and the output voltage waveform is almost a square wave, not a sawtooth wave. The shape of the output waveform can be further optimized by adjusting its frequency or using different

memristor parameters. The transient behavior of the MBSSG generator for 250 Hz can be seen in Figure 10 while as its steady-state behavior for 250 Hz is shown in Figure 9. The memristor state variable switches from 0 to 1 or 1 to 0 if the half period of the input square wave signal is higher than the resistive switching time as shown in Figure 7. The output waveform rises quickly and gets fixed at the value $(V_{sat} R_{off})/R_2$ in the positive alternance and the output waveform falls quickly and gets fixed at the value $-(V_{sat} R_{on})/R$ in Figure 7. However, if the half period of the square wave signal is lower than the resistive switching time, the resistive switching cannot be completed as shown in Figures 8 and 9. Over 250 Hz or at very high frequencies, the memristor starts behaving as if a linear time-invariant resistor, and, therefore, the MBSSG generator starts giving a square waveform. That's why the middle frequencies are the best for the operation of the MBSSG since the waveform resembles a sawtooth the most.

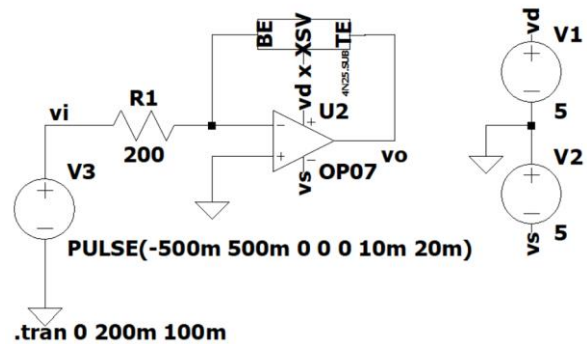


Figure 6. The LTspice schematic of the inspected generator.

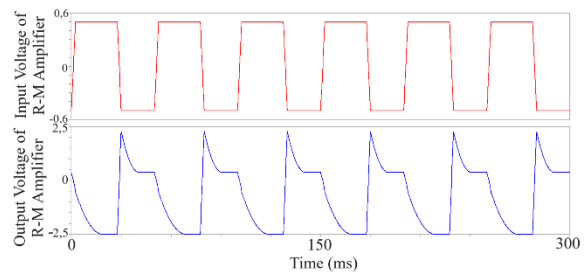


Figure 7. a) Input and b) Output Voltages of the R-M Inverting Amplifier for 20 Hz Input Frequency (

$R_2=200 \Omega$, $x(0)=0.076$, and the memristor model parameters same as Table 1)

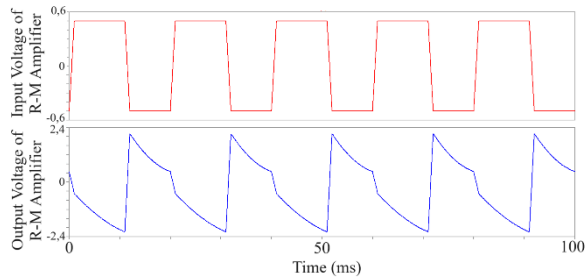


Figure 8. a) Input and b) Output Voltages of the R-M Inverting Amplifier for 50 Hz Input Frequency ($R_2=200 \Omega$, $x(0)=0.076$, and the memristor model parameters same as Table 1)

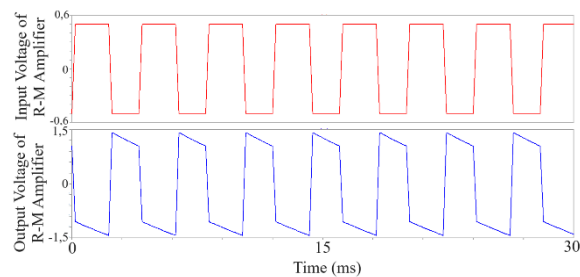


Figure 9. a) Input and b) Output Voltages of the R-M Inverting Amplifier for 250 Hz Input Frequency ($R_2=200 \Omega$, $x(0)=0.076$, and the memristor model parameters same as Table 1)

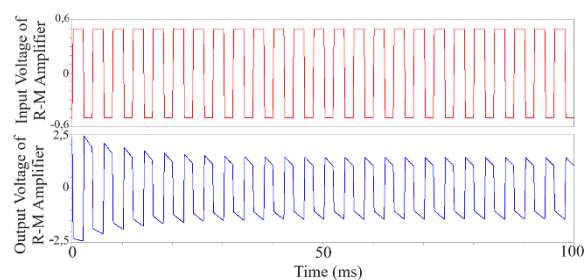


Figure 10. a) Input and b) Output Voltages of the R-M Inverting Amplifier for 250 Hz Input Frequency ($R_2=200 \Omega$, $x(0)=0.076$, and the memristor model parameters same as Table 1)

5. Conclusion

New circuit elements require models to be used in circuit programs such as Spice. Memristor is a

nonlinear element that has emerged in recent decades. A new window function, which gives finite resistive switching times has been reported in (Mutlu & Kumru, 2023). In this paper, an LTspice model of Mutlu-Kumru memristor model is presented and used to model a memristor-based sawtooth signal generator. The solutions with window functions given in (Kurt Demir A.; Mutlu R., 2019) are not valid due to boundary-tackling and boundary unreachability issues. The analytical solution of the generator has also been made to show that the signal generator is analytically solvable with Mutlu-Kumru window function.

In the future, once memristors are commercially available, it may be feasible to develop various types of signal generators based on memristors. However, inaccurate modeling of a memristor can lead to errors in these analog application circuits as well. Therefore, companies intending to commercialize memristors should also provide SPICE circuit models that accurately represent them to facilitate their integration into circuits.

Conflict of Interest: The authors declare no conflict of interest to be disclosed.

ORCID

Ertuğrul Karakulak, 0000-0001-5937-2114

Reşat Mutlu, 0000-0003-0030-7136

References

- Ascoli, A., Tetzlaff, R., Corinto, F., Mirchev, M., & Gilli, M. (2013). Memristor-based filtering applications. *LATW 2013 - 14th IEEE Latin-American Test Workshop*, 1, 1–6. <https://doi.org/10.1109/LATW.2013.6562672>
- Berdan, R.; Prodromakis, T.; Toumazou, C. (2012). High precision analogue memristor state tuning. *Electronics Letters*, 48(18), 1105–1107.
- Biolek, Z., Biolek, D., & Biolková, V. (2009). SPICE model of memristor with nonlinear dopant drift. *Radioengineering*, 18(2), 210–214.

- Chua, L. (2011). Resistance switching memories are memristors. *Applied Physics A*, 102(4), 765–783. <https://doi.org/10.1007/s00339-011-6264-9>
- Chua, L. O. (1971). Memristor—The Missing Circuit Element. *IEEE Transactions on Circuit Theory*, 18(5), 507–519. <https://doi.org/10.1109/TCT.1971.1083337>
- Chua, L. O., & Kang, S. M. (1976). Memristive Devices and Systems. *Proceedings of the IEEE*, 64(2), 209–223. <https://doi.org/10.1109/PROC.1976.10092>
- Eroğlu, Y. O. A. F. G. A. H. (2017). A new window function for memristor modeling. 8th International Advanced Technologies Symposium, 3498–3502.
- Hernández-Mejía, C., & Torres-Muñoz, D. (2019, February). PWL Window Function for Nonlinear Memristive Systems. In 2019 International Conference on Electronics, Communications and Computers (CONIELECOMP) (pp. 9-13). IEEE.
- Itoh, M., & Chua, L. O. (2008). Memristor oscillators. *International Journal of Bifurcation and Chaos*, 18(11), 3183–3206. <https://doi.org/10.1142/S0218127408022354>
- Joglekar, Y. N., & Wolf, S. J. (2009). The elusive memristor: Properties of basic electrical circuits. *European Journal of Physics*, 30(4), 661–675. <https://doi.org/10.1088/0143-0807/30/4/001>
- Karakulak, E., & Mutlu, R. (2020). Spice model of current polarity-dependent piecewise linear window function for memristors. *Gazi University Journal of Science*, 33(4), 766–777. <https://doi.org/10.35378/gujs.605118>
- Khalid, M. (2019). Review on Various Memristor Models, Characteristics, Potential Applications, and Future Works. *Transactions on Electrical and Electronic Materials*, 20(4), 289–298. <https://doi.org/10.1007/s42341-019-00116-8>
- Kvatinsky, S., Friedman, E. G., Kolodny, A., & Weiser, U. C. (2012). TEAM: Threshold adaptive memristor model. *IEEE transactions on circuits and systems I: regular papers*, 60(1), 211–221.
- Kurtdemir A.; Mutlu R. (2019). Modeling and Simulation of a Memristor-Based Sawtooth Signal Generator Using Nonlinear Dopant Drift Memristor Models. *European Journal of Engineering and Applied Sciences*, 2(1), 44–57.
- Mosad, a. G., Fouda, M. E., Khatib, M. a., Salama, K. N., & Radwan, a. G. (2013). Improved memristor-based relaxation oscillator. *Microelectronics Journal*, 44(9), 814–820. <https://doi.org/10.1016/j.mejo.2013.04.005>
- Muthuswamy, B. (2010). Implementing memristor based chaotic circuits. *International Journal of Bifurcation and Chaos*, 20(5), 1335–1350. <https://doi.org/10.1142/S0218127410026514>
- Mutlu, R., Karakulak, E. (2018). Memristor-Based Phase Shifter. 2018 2nd International Symposium on Multidisciplinary Studies and Innovative Technologies (ISMSIT), 1–5.
- Mutlu, R. (2015). Solution of TiO₂ memristor-capacitor series circuit excited by a constant voltage source and its application to calculate operation frequency of a programmable TiO₂ memristor-capacitor relaxation oscillator. *Turkish Journal of Electrical Engineering and Computer Sciences*, 23(5), 1219–1229. <https://doi.org/10.3906/elk-1108-38>
- Mutlu, R., & Kumru, T. D. (2023). A Zeno Paradox: Some Well-known Nonlinear Dopant Drift Memristor Models Have Infinite Resistive

- Switching Time. *Radioengineering*, 32(3), 312–324. <https://doi.org/10.13164/RE.2023.0312>
- Oğuz, Y., Gül, F., Eroğlu, H., “A New Window Function for Memristor Modeling”, 8th International Advanced Technologies Symposium, (2017).
- Özgüvenç, A., Mutlu, R., & Karakulak, E. (2016). Sawtooth signal generator with a memristor. 1st International Conference on Engineering Technology and Applied Sciences, April, 19–24.
- Pershin, Y. V., & Di Ventra, M. (2010). Practical approach to programmable analog circuits with memristors. *IEEE Transactions on Circuits and Systems I: Regular Papers*, 57(8), 1857–1864. <https://doi.org/10.1109/TCSI.2009.2038539>
- Pershin, Y. V., & Di Ventra, M. (2011). Memory effects in complex materials and nanoscale systems. In *Advances in Physics* (Vol. 60, Issue 2, pp. 145–227). <https://doi.org/10.1080/00018732.2010.544961>
- Pershin, Y. V., Martinez-Rincon, J., & Di Ventra, M. (2011). Memory circuit elements: From systems to applications. *Journal of Computational and Theoretical Nanoscience*, 8(3), 441–448. <https://doi.org/10.1166/jctn.2011.1708>
- Prodromakis, T., Peh, B. P., Papavassiliou, C., & Toumazou, C. (2011). A versatile memristor model with nonlinear dopant kinetics. *IEEE Transactions on Electron Devices*, 58(9), 3099–3105. <https://doi.org/10.1109/TED.2011.2158004>
- Prodromakis, T., & Toumazou, C. (2010). A review on memristive devices and applications. 2010 IEEE International Conference on Electronics, Circuits, and Systems, ICECS 2010 - Proceedings, 934–937. <https://doi.org/10.1109/ICECS.2010.5724666>
- Shin, S., Kim, K., & Kang, S. M. (2009). Memristor-based fine resolution programmable resistance and its applications. 2009 International Conference on Communications, Circuits and Systems, ICCAS 2009, 948–951. <https://doi.org/10.1109/icccas.2009.5250376>
- Shin, S., Kim, K., & Kang, S. M. (2011). Memristor applications for programmable analog ICs. *IEEE Transactions on Nanotechnology*, 10(2), 266–274. <https://doi.org/10.1109/TNANO.2009.2038610>
- Strukov, D. B., Snider, G. S., Stewart, D. R., & Williams, R. S. (2008). The missing memristor found. *Nature*, 453(7191), 80–83. <https://doi.org/10.1038/nature06932>
- Talukdar, A., Radwan, A. G., & Salama, K. N. (2011). Generalized model for Memristor-based Wien family oscillators. *Microelectronics Journal*, 42(9), 1032–1038. <https://doi.org/10.1016/j.mejo.2011.07.001>
- Wey, T. A., & Benderli, S. (2009). Amplitude modulator circuit featuring TiO₂ memristor with linear dopant drift. *Electronics Letters*, 45(22), 1103–1104. <https://doi.org/10.1049/el.2009.2174>
- Wey, T. a., & Jemison, W. D. (2011). Variable gain amplifier circuit using titanium dioxide memristors. *IET Circuits, Devices & Systems*, 5(1), 59. <https://doi.org/10.1049/iet-cds.2010.0210>
- Yener, S. Ç., Mutlu, R., & Kuntman, H. (2014). A new memristor-based high-pass filter/amplifier: Its analytical and dynamical models. 2014 24th International Conference Radioelektronika, RADIOELEKTRONIKA 2014 - Proceedings. <https://doi.org/10.1109/Radioelek.2014.6828420>

- Yener, S. C., Mutlu, R., & Kuntman, H. H. (2018). Small signal analysis of memristor-based low-pass and high-pass filters using the perturbation theory. *Optoelectronics and Advanced Materials, Rapid Communications*, 12(1–2), 55–62.
- Yener, Ş. Ç., Mutlu, R., & Kuntman, H. H. (2014). Performance analysis of a memristor - Based biquad filter using a dynamic model. *Informacije MIDEM*, 44(2), 109–118.
- Zha, J., Huang, H., & Liu, Y. (2016). A Novel Window Function for Memristor Model with Application in Programming Analog Circuits. *IEEE Transactions on Circuits and Systems II: Express Briefs*, 63(5), 423–427. <https://doi.org/10.1109/TCSII.2015.2505959>